Inorganic Chemistry

Article

pubs.acs.org/IC

A $Mn^{II}_6Mn^{III}_6$ Single-Strand Molecular Wheel with a Reuleaux Triangular Topology: Synthesis, Structure, Magnetism, and DFT Studies

Sotiris Zartilas,[†] Constantina Papatriantafyllopoulou,[†] Theocharis C. Stamatatos,[‡,§] Vassilios Nastopoulos,[⊥] Eduard Cremades,[∥] Eliseo Ruiz,[∥] George Christou,[‡] Christos Lampropoulos,[†,#] and Anastasios J. Tasiopoulos*[,†]

[†]Department of Chemistry, University of Cyprus, 1678 Nicosia, Cyprus

[‡]Department of Chemistry, University of Florida, Gainesville, Florida 32611, United States

[⊥]Department of Chemistry, University of Patras, Patras 26504, Greece

[∥]Department de Química Inorgànica and Institut de Recerca de Química Teòrica i Computacional, Universitat de Barcelona, Diagonal 645, 08028 Barcelona, Spain

[#]Department of Chemistry, University of North Florida, Jacksonville, Florida 32224, United States

Supporting Information

ABSTRACT: The use of the anion of 3-methyl-1,3,5-pentanetriol (mpt^{3-}) in manganese carboxylate chemistry has afforded the new $Mn^{II/III}_{12}$ cluster $[Mn^{II}_6Mn^{III}_6(mpt)_6(CH_3CO_2)_{12}(py)_6]\cdot 3CH_3CN$ (**1**·3CH_3CN). Complex **1** was isolated in moderate yield by the reaction of $Mn(CH_3CO_2)_2\cdot 4H_2O$ and H_3mpt in a 2.6:1 molar ratio in a solvent mixture of acetonitrile and pyridine. The structure of **1** consists of alternating $[Mn^{II}_2(CH_3CO_2)_3(py)]^+$ and $[Mn^{III}_2(\mu\text{-}OR)_2(CH_3CO_2)(py)]^{3+}$ dimeric units (three of each dimer), linked at each end by two alkoxo and one acetate bridges; the mpt^{3-} ligands adopt the $\eta^2{:}\eta^2{:}\eta^2{:}\mu_4$ coordination mode. The overall metal topology of this new Mn_{12} wheel resembles a guitar plectrum, or a Reuleaux triangle. Complex **1** displays an unprecedented structural topology, being the first example of a $Mn^{II}_6Mn^{III}_6$ wheel constructed from alternating homovalent dimers and the only known Mn_{12} loop with the trigonal symmetry of a Reuleaux triangle (all other reported loops were ellipsoids). Variable-temperature, solid-state direct- and alternating-current magnetization studies were carried out on complex **1**, revealing the presence of antiferromagnetic exchange interactions between the metal ions in the molecule, which lead to a spin ground-state value $S = 0$; the exchange coupling parameters J were calculated using density functional theory employing a hybrid B3LYP functional.

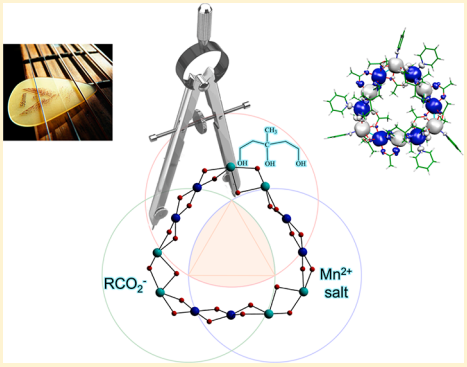

INTRODUCTION

Molecular 3d metal cluster chemistry has been flourishing during the past few decades, owing to the intense interdisciplinary research efforts for the understanding of the mesoscopic regime, for which relatively little is known; thus, condensed-matter physicists are eagerly searching for useful models to probe mesoscopic phenomena. Polynuclear transition-metal clusters have been serving as such models.[1] These clusters are also interesting because of (a) their aesthetically pleasing structures/architectures and (b) their relevance to a variety of other fields, such as bioinorganic chemistry[2−5] and molecular magnetism. In the field of molecular magnetism, some 3d metal clusters are single-molecule magnets (SMMs),[6] behaving as superparamagnets and exhibiting magnetization hysteresis below a blocking temperature T_B. Their properties originate from the intrinsic structural and electronic characteristics of their metal cores, and their potential applications range from high-density information storage, to molecular spintronics,[7] and to qubits for quantum computation.[8] Additionally, several other quantum-mechanical phenomena have been identified in SMMs, such as spin−phonon coupling,[9] spin-state entanglement,[8] spin parity,[10] both thermally assisted and pure quantum tunneling of the magnetization,[11] quantum phase interference,[10b,12] and others.[13]

Therefore, it is clear that in order to probe complicated mesoscopic phenomena the need for model compounds is continually increasing. Even though SMM/cluster chemistry is still an attractive area, our interest has been recently extended to toroidal compounds; such wheel-type 3d metal complexes have a number of precedents in the literature, including high-nuclearity multilayer or cluster-based wheels,[14] single-stranded homo- and heterometallic wheels,[15] and others. A small number of molecular wheels are single-stranded and typically

Received: July 23, 2013
Published: October 4, 2013

   dx.doi.org/10.1021/ic401872c | *Inorg. Chem.* 2013, 52, 12070−12079

antiferromagnetic, some of which were proposed as candidate model compounds for investigations on the origins of magnetic anisotropy,[16] as well as probes of the Néel vector coherent tunneling mechanism.[17] Quantum coherence occurs when energy exchange with the environment is not required for a material to oscillate between the "spin-up" and "spin-down" states. The observation of the orientation change of a spin vector, which induces the spin-flip of all other spin carriers in the ring, is evidence of the Néel vector reversal; at low temperatures, this is expected to occur coherently by a tunneling mechanism.[18] Molecular wheels are also good models for the study of 1D magnetism,[19,20] spin frustration[21] (antiferromagnetic odd-numbered wheels), and host–guest chemistry.[22] Finding good model systems for such complicated phenomena is a formidable task, and thus wheels constitute an attractive class of compounds.

Even though homovalent wheels are common for many trivalent 3d metal ions, with several examples including wheels of V^{III},[23] Cr^{III},[24] Mn^{III},[25] Fe^{III},[26] and Ga^{III},[27] mixed-valent wheels are rare.[14d,15a,28,29] One family of manganese wheels has the general formula $[Mn_{12}(L)_8(RCO_2)_{14}]$,[28,30] where L are various N-substituted diethanolamine dianions and R = Me, Et. These compounds consist of six Mn^{II} and six Mn^{III} ions, arranged in an alternating fashion in the loop and possess a spin ground state of $S = 7$;[31] such Mn_{12} loops are also rare examples of wheel-shaped SMMs. Additionally, the organization of the metal centers in the mixed-valent Mn_{12} wheels in theory allows for antisymmetric exchange coupling between spins, that is, the Dzyaloshinskii–Moriya (DM) interaction;[32] the latter can lift the degeneracy of energy level crossings belonging to different spin multiplets and allow for tunneling and interference between these levels. Indeed, it was recently proven that the tunneling transitions and quantum phase interference in Mn_{12} wheel SMMs were strongly dependent on the direction of the DM vector.[33]

Herein, we report the synthesis, crystal structure, and magnetic properties of a new Mn_{12} wheel-shaped complex, namely, $[Mn_{12}(mpt)_6(CH_3CO_2)_{12}(py)_6]\cdot 3CH_3CN$ (**1**·$3CH_3CN$), where mpt^{3-} is the trianion of 3-methyl-1,3,5-pentanetriol (Scheme 1). To the best of our knowledge, this is only the second example of a metal complex incorporating this ligand.[34] Complex **1** is relevant to the family of Mn_{12} wheels discussed above since it also contains six Mn^{II} and six Mn^{III} ions but with different shape and symmetry because of the relative positions of the Mn^{II} and Mn^{III} ions in **1**. Furthermore, direct-current (dc) and alternating-current (ac) magnetic susceptibility studies are reported, accompanied by density functional theory (DFT) calculations for determination of the exchange parameters.

Scheme 1. 3-Methyl-1,3,5-pentanetriol (H_3mpt) Ligand Used in This Study

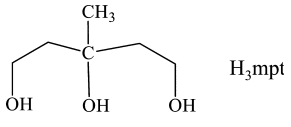

EXPERIMENTAL SECTION

Synthesis. All manipulations were performed under aerobic conditions using materials as received.

$[Mn_{12}(mpt)_6(CH_3CO_2)_{12}(py)_6]\cdot 3CH_3CN$ (1·$3CH_3CN$). A colorless solution of H_3mpt (0.039 mL, 0.043 g, 0.32 mmol) in CH_3CN/py (20:3, v/v; 10 mL) was added to a solution of $Mn(CH_3CO_2)_2\cdot 4H_2O$ (0.200 g, 0.82 mmol) in CH_3CN/py (20:3, v/v; 10 mL). The resulting red-orange solution was stirred for approximately 30 min at room temperature. A small quantity of undissolved material was removed by filtration, and the filtrate was left undisturbed in a sealed flask. After 10 days, X-ray quality reddish-brown crystals of **1**·$3CH_3CN$ were collected by filtration, washed with MeCN (2 × 5 mL) and Et_2O (2 × 5 mL), and dried under vacuum; the yield was 0.08 g; the vacuum-dried solid analyzed as **1**·H_2O. Anal. Calcd (found) for $C_{90}H_{134}N_6O_{43}Mn_{12}$: C, 40.84 (41.05); H, 5.10 (4.86); N, 3.17 (3.30). Selected IR data (cm^{-1}): 2920 (sm), 2847 (m), 1558 (s), 1408 (s), 1286 (w), 1182 (mw), 1124 (s), 1074 (s), 933 (s), 874 (s), 743 (w), 662 (s), 581 (s), 449 (w).

X-ray Crystallography. Data were collected on an Oxford Diffraction Xcalibur diffractometer equipped with a CCD area detector and a graphite monochromator utilizing Mo Kα radiation (λ = 0.71073 Å). A suitable crystal of **1**·$3CH_3CN$ was attached to the glass fiber using paratone-N oil and transferred to a goniostat, where it was cooled to 100 K for data collection. Unit cell dimensions were determined and refined using 16778 reflections ($3.02 \leq \theta \leq 30.47$). Empirical absorption corrections (multiscan based on symmetry-related measurements) were applied using *CrysAlisRED* software.[35] The structure was solved by direct methods using *SIR92*[36a] and refined on F^2 with full-matrix least squares using *SHELXL97*.[36b] Software packages used: *CrysAlisCCD*[35] for data collection, *CrysAlisRED*[35] for cell refinement and data reduction; *WINGX*[36c] for geometric calculations; *DIAMOND*[37a] and *MERCURY*[37b] for molecular graphics. The non-H atoms were treated anisotropically, whereas the H atoms were placed in calculated, ideal positions and refined as riding on their respective C atoms. Unit cell parameters and structure solution and refinement data for complex **1**·$3CH_3CN$ are listed in Table 1.

Physical Studies. IR spectra were recorded in the solid state (KBr pellets) on a Shimadzu Prestige-21 spectrometer in the 4000–400 cm^{-1} range. Variable-temperature dc and ac magnetic susceptibility data were collected at the University of Florida using a Quantum

Table 1. Crystallographic Data for Complex 1·3MeCN

	1·3MeCN
formula[a]	$C_{96}H_{141}N_9Mn_{12}O_{42}$
fw,[a] g mol^{-1}	2752.46
cryst syst	trigonal
space group	*R*3*c*
a, Å	33.736(2)
b, Å	33.736(2)
c, Å	17.8948(7)
α, deg	90.00
β, deg	90.00
γ, deg	120.00
V, $Å^3$	17637(2)
Z	6
T, K	100(2)
radiation, Å	0.71073[b]
ρ_{calcd}, g cm^{-3}	1.555
μ, mm^{-1}	1.326
measd/unique reflns	77469/6867
R_{int}	0.1037
obsd reflns	5090
R1[c]	0.0385
wR2[d]	0.0639
GOF on F^2	1.087
$\Delta\rho_{max}$, $\Delta\rho_{min}$, e $Å^{-3}$	0.473, −0.364

[a]Including solvate molecules. [b]Mo Kα radiation. [d]R1 = $\sum(||F_o| - |F_c||)/\sum|F_o|$. [c]For observed $[I > 2\sigma(I)]$ reflections. [d]wR2 = $[\sum[w(F_o^2 - F_c^2)^2]/\sum[w(F_o^2)^2]]^{1/2}$, $w = 1/[\sigma^2(F_o^2) + (ap)^2 + bp]$, where $p = [\max(F_o^2,0) + 2F_c^2]/3$.

dx.doi.org/10.1021/ic401872c | *Inorg. Chem.* 2013, 52, 12070–12079

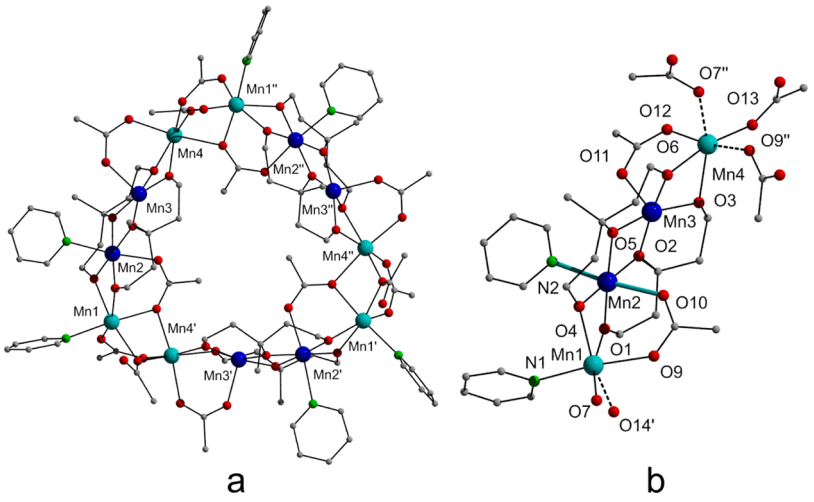

Figure 1. Partially labeled representations of (a) the molecular structure of complex **1** and (b) the repeating (asymmetric) $[Mn^{II}_2Mn^{III}_2(mpt)_2(py)_2(CH_3CO_2)_2]^{2+}$ unit of complex **1**. H atoms have been omitted for clarity. The dashed bonds denote connections to the neighboring repeating unit. The thicker aqua bond denotes the JT axes on the six-coordinate Mn^{III} ion. Color code: Mn^{II}, turquoise; Mn^{III}, blue; N, green; O, red; C, gray.

Design MPMS-XL SQUID susceptometer equipped with a 7 T magnet and operating in the 1.8−300 K range. Samples were embedded in solid eicosane to prevent torquing. The ac magnetic susceptibility measurements were performed in an oscillating ac field of 3.5 G and a zero dc field. The oscillation frequencies were in the 5−1488 Hz range. Pascal's constants were used to estimate the diamagnetic corrections, which were subtracted from the experimental susceptibilities to give the molar paramagnetic susceptibility (χ_M). Elemental analyses (C, H, and N) were performed by the in-house facilities of the Chemistry Department at the University of Florida.

Computational Details. For calculation of the exchange coupling constants for any polynuclear complex with n different exchange constants, the energy of at least $n + 1$ spin configurations must be calculated.[38] If more energy values are calculated, a fitting procedure is required to extract the J values. In the case of the studied complex, to obtain the four J values, seven spin configurations have been used: (i) the high-spin solution ($S = 27$); (ii) two $S = 15$ distributions with the inversion of three Mn^{III} spins at {Mn3, Mn3′, Mn3″} and {Mn2, Mn2′, Mn2″} (see Figure 1) in the first and second distributions, respectively; (iii) one $S = 14$ distribution with the inversion of spins at {Mn3″, Mn2′, Mn1′}; (iv) two $S = 12$ distributions with the inversion of three Mn^{II} spins at {Mn1, Mn1′, Mn1″} and {Mn4′, Mn4″, Mn4} in the first and second distributions, respectively; (v) an $S = 1$ distribution with the inversion of spins at {Mn3, Mn3″, Mn2, Mn2″, Mn1, Mn1″}. A more detailed description of the procedure used to obtain the exchange parameter constants has been reported elsewhere.[39] The calculations have been performed with the B3LYP functional[40] together with the *NWChem* code (version 5.1)[41] and a guess function generated with the *Jaguar* 7.5 code.[42] Finally, the triple-ζ all-electron Gaussian basis set proposed by Schaefer et al. was employed.[43]

RESULTS AND DISCUSSION

Synthesis. Our group has been investigating the employment of diol-type ligands, such as 1,3-propanediol (H_2pd) and 2-methyl-1,3-propanediol (H_2mpd), in manganese carboxylate chemistry as a route to new polynuclear clusters and SMMs. The anionic form of these ligands contains two alkoxide arms, which favor the formation of polynuclear products and thus have been proven to be a rich source of high-nuclearity Mn clusters and SMMs.[14e−g,44] This investigation recently expanded to include ligands with more ROH groups, in order to study the effect of higher linking ability on the nuclearity and magnetic properties of the resulting products. A suitable ligand for this study seemed to be 3-methyl-1,3,5-pentanetriol (H_3mpt), which contains three ROH arms (Scheme 1); to the best of our knowledge, the only other 3d metal cluster bearing this tridentate ligand is the mixed-valent cation $[Mn^{III}_6Mn^{II}_4O_4(Hmpt)_6(N_3)_3Br_2]^+$ exhibiting a supertetrahedral $[Mn^{III}_6Mn^{II}_4O_4]^{18+}$ structural core.[34]

Various reactions have been systematically explored with differing reagent ratios, reaction solvents, and other conditions. The reaction of $Mn(CH_3CO_2)_2{\cdot}4H_2O$ and H_3mpt in a 2.6:1 molar ratio in CH_3CN/py (20:3, v/v) afforded a red-orange solution from which compound **1**·3CH_3CN was subsequently isolated. The formation of complex **1** is summarized in eq 1.

$$12Mn(CH_3CO_2)_2 + 6H_3mpt + 6py + \frac{3}{2}O_2 \xrightarrow{MeCN/py} \underset{\mathbf{1}}{[Mn_{12}(mpt)_6(CH_3CO_2)_{12}(py)_6]} + 12CH_3CO_2H + 3H_2O \quad (1)$$

The reaction involves Mn oxidation, undoubtedly by O_2 under the prevailing basic conditions, and has been balanced accordingly. The $CH_3CO_2^-$ ions act as both proton acceptors, facilitating formation of the mpt^{3-} anion, and bridging ligands, playing a key role in formation of the Mn_{12} complex. Alteration of the solvent ratio did not affect the product identity, whereas when the reaction was performed in the absence of pyridine, an insoluble powder that could not be further characterized was isolated. Small variations in the Mn^{II}/H_3mpt ratio did not either affect the identity of the product or increase the yield of the reaction any further. We investigated the possibility of synthesizing complex **1** from different solvent combinations to target the incorporation of different terminal groups; however, the solid/polycrystalline precipitates were mixtures, possibly of **1** contaminated by other unidentifiable solid byproducts.

Description of the Structure. The partially labeled structure of complex **1** is shown in Figure 1a, while the labeled asymmetric unit of **1** is presented in Figure 1b; selected interatomic distances and angles for **1** are listed in Table 2.

The structure of **1** (Figure 1a) comprises six Mn^{II} and six Mn^{III} ions linked through $CH_3CO_2^-$ and mpt^{3-} bridges to form

dx.doi.org/10.1021/ic401872c | *Inorg. Chem.* 2013, 52, 12070−12079

Table 2. Selected Interatomic Distances (Å) and Angles (deg) for Complex 1[a]

Mn1−O1	2.188(3)	Mn3−O2	1.911(3)
Mn1−O4	2.165(3)	Mn3−O3	1.867(3)
Mn1−O7	2.148(3)	Mn3−O5	1.913(3)
Mn1−O9	2.244(3)	Mn3−O6	1.845(3)
Mn1−O14″	2.132(3)	Mn3−O11	2.114(3)
Mn1−N1	2.265(4)	Mn4−O3	2.181(3)
Mn2−O1	1.856(3)	Mn4−O6	2.188(4)
Mn2−O2	1.927(3)	Mn4−O7″	2.166(4)
Mn2−O4	1.865(3)	Mn4−O9″	2.209(3)
Mn2−O5	1.937(3)	Mn4−O12	2.167(4)
Mn2−O10	2.246(4)	Mn4−O13	2.102(4)
Mn2−N2	2.322(4)	Mn1···Mn2	3.084(1)
Mn2···Mn3	2.913(1)	Mn3···Mn4	3.069(1)
O1−Mn1−O4	69.7(2)	O5−Mn2−N2	90.8(2)
O1−Mn1−O7	166.7(2)	O10−Mn2−N2	174.1(2)
O1−Mn1−O9	89.0(2)	O2−Mn3−O3	96.7(2)
O1−Mn1−O14″	86.9(2)	O2−Mn3−O5	80.9(2)
O1−Mn1−N1	93.2(2)	O2−Mn3−O6	170.6(2)
O4−Mn1−O7	112.5(2)	O2−Mn3−O11	93.9(2)
O4−Mn1−O9	91.1(2)	O3−Mn3−O5	162.3(2)
O4−Mn1−O14″	156.6(2)	O3−Mn3−O6	84.0(2)
O4−Mn1−N1	95.0(2)	O3−Mn3−O11	93.9(2)
O7−Mn1−O9	78.0(2)	O5−Mn3−O6	95.5(2)
O7−Mn1−O14″	90.1(2)	O5−Mn3−O11	103.7(2)
O7−Mn1−N1	99.5(2)	O6−Mn3−O11	95.4(2)
O9−Mn1−O14″	87.5(2)	O3−Mn4−O6	69.3(2)
O9−Mn1−N1	173.9(2)	O3−Mn4−O7″	159.9(2)
O14″−Mn1−N1	86.9(2)	O3−Mn4−O9″	104.1(2)
O1−Mn2−O2	97.8(2)	O3−Mn4−O12	84.1(2)
O1−Mn2−O4	83.9(2)	O3−Mn4−O13	102.4(2)
O1−Mn2−O5	177.3(2)	O6−Mn4−O7″	91.2(2)
O1−Mn2−O10	93.6(2)	O6−Mn4−O9″	86.8(2)
O1−Mn2−N2	90.7(2)	O6−Mn4−O12	96.5(2)
O2−Mn2−O4	176.5(2)	O6−Mn4−O13	168.9(2)
O2−Mn2−O5	79.9(2)	O7″−Mn4−O9″	78.4(2)
O2−Mn2−O10	83.7(2)	O7″−Mn4−O12	94.1(2)
O2−Mn2−N2	91.7(2)	O7″−Mn4−O13	97.6(2)
O4−Mn2−O5	98.3(2)	O9″−Mn4−O12	171.8(2)
O4−Mn2−O10	93.2(2)	O9″−Mn4−O13	88.3(2)
O4−Mn2−N2	91.4 (2)	O12−Mn4−O13	89.8(2)
O5−Mn2−O10	84.8(2)		

[a]Symmetry code: ′ = 2 − *y*, 1 + *x* − y, *z*; ″ = 1 − *x* + y, 2 − *x*, *z*.

a puckered, single-stranded wheel of virtual C_3 point group symmetry. It can be conveniently described as a guitar plectrum, or a regular Reuleaux triangle of $[Mn^{II}_2Mn^{III}_2(mpt)_2(py)_2(CH_3CO_2)_2]^{2+}$ units (Figure 1b), linked at each end by three bridging $CH_3CO_2^-$ groups. The π-optimal or so-called regular Reuleaux triangle (the equivalent of a C_3-symmetric triangle) is the simplest Reuleaux polygon; such polygons have an odd number of vertices, which are based on curves of identical width.[45] Similarly, complex **1** consists of three curves of constant width, each including the $[Mn^{II}_2Mn^{III}_2(mpt)_2(py)_2(CH_3CO_2)_2]^{2+}$ unit, with the distance between the first and fourth Mn ion in each unit (Mn1 and Mn4) being 8.79 Å and the dihedral angle defined by the four Mn−Mn bond vectors (Mn1−Mn2−Mn3−Mn4) within each tetranuclear unit being 2.67°. There are two $\eta^2{:}\eta^2{:}\eta^2{:}\mu_4$ mpt^{3-} ligands (Figure 2a) in each unit, bridging the four Mn atoms,

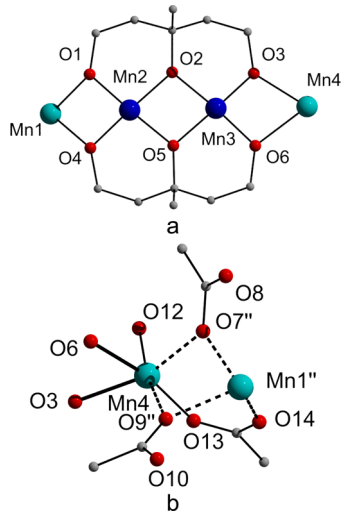

Figure 2. Partially labeled representations of (a) the $\eta^2{:}\eta^2{:}\eta^2{:}\mu_4$ binding mode of the mpt^{3-} ligands and (b) the connection or "hinge" between two neighboring units or "struts". The dashed bonds denote connections to the neighboring repeating unit. Color code: Mn^{II}, turquoise; Mn^{III}, blue; O, red; C, gray.

namely, Mn1−4 and their symmetry-related partners. The neighboring Mn^{II}−Mn^{III} pairs of the asymmetric unit (Mn4−Mn3 and Mn1−Mn2) are additionally bridged by one acetate ion each, which in the case of Mn4−Mn3 pair adopts its familiar $\eta^1{:}\eta^1{:}\mu$ (syn,syn) mode oriented toward the exterior of the loop. The acetate linking the Mn1−Mn2 ions is pointed toward the center of the loop adopting the $\eta^1{:}\eta^2{:}\mu_3$ coordination mode and bridges these ions to a Mn^{II} atom (Mn4 and its symmetry equivalents) of a neighboring Mn_4 unit. Thus, $\eta^1{:}\eta^2{:}\mu_3$ $CH_3CO_2^-$, together with $\eta^2{:}\mu$ and $\eta^1{:}\eta^1{:}\mu$ $CH_3CO_2^-$ ions, which are located outside the loop, act as the "hinges" between two adjacent structural subunits (Figure 2b), which, in turn, can be imagined as the "struts" of the overall structure. Alternatively, the structure of **1** can be described as consisting of repeating homovalent dinuclear $[Mn^{II}_2(CH_3CO_2)_3(py)]^+$ and $[Mn^{III}_2(\mu\text{-}OR)_2(CH_3CO_2)(py)]^{3+}$ units linked at each end by two alkoxo and one acetate bridges.

The Mn^{II} ions (Mn1, Mn4, and their symmetry equivalents) and one of the two Mn^{III} centers of each unit (Mn2 and its symmetry partners) are six-coordinate, exhibiting a near-octahedral geometry. The remaining Mn^{III} ion (Mn3 and its symmetry equivalents) is five-coordinate with a distorted square-pyramidal coordination geometry; the O11 atom from an $\eta^1{:}\eta^1{:}\mu$ $CH_3CO_2^-$ group occupies the axial position. The $Mn^{II/III}$ oxidation states were established through charge considerations, bond-valence-sum (BVS) calculations (Table 3),[46] and the clear Jahn−Teller (JT) distortions of the six-

Table 3. BVS Calculations for the Mn Ions in Complex 1

atom[a]	Mn^{II}	Mn^{III}	Mn^{IV}
Mn1	<u>1.93</u>	1.75	1.84
Mn2	3.31	<u>3.03</u>	3.18
Mn3	3.30	<u>3.01</u>	3.17
Mn4	<u>2.02</u>	1.85	1.94

[a]The underlined value is the one closest to the charge for which it was calculated. The oxidation state can be taken as the whole number nearest to the underlined value.

dx.doi.org/10.1021/ic401872c | *Inorg. Chem.* 2013, 52, 12070−12079

coordinate Mn^{III} ions, which take the form of axial elongation of the N2−Mn2−O10 and its symmetry related axes. The Mn2−O10 bond measures 2.246(4) Å and the Mn2−N2 bond 2.322(4) Å; as expected for a d^4 metal ion in octahedral geometry, these axial bonds are distinctly longer than the equatorial ones, which range between 1.856(3) and 1.937(3) Å. Note that the angle between the JT axis and the mean plane defined by the 12 Mn atoms is 68.0°, while the angle between two different JT axes (approximated as the mean JT axis vector) is ∼73.2°.

The Mn_{12} ring deviates from planarity, with Mn1, Mn2, and their symmetry-related partners lying 0.3093 and 0.3947 Å, respectively, below the mean plane of the 12 Mn atoms and Mn3, Mn4, and their symmetry counterparts lying 0.0039 and 0.5888 Å above the same plane, respectively.

The unit cell of **1** contains a single orientation of the Mn_{12} wheel. A packing diagram is presented in Figure 3. The

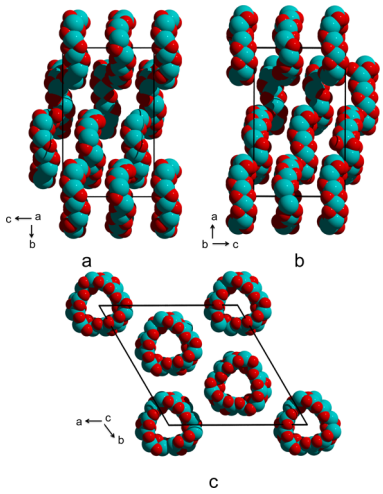

Figure 3. Crystal packing diagram of the Mn−O core of **1** depicted along the crystallographic (a) *a*, (b) *b*, and (c) *c* axes. Color code: Mn, turquoise; O, red.

molecules pack in a columnar fashion, with the stacking directions being parallel to the shortest unit cell axis *c*. There are no significant intra- or intermolecular hydrogen-bonding interactions, suggesting that each molecule is essentially isolated from its neighbors, as revealed from the relatively large Mn···Mn separations between neighboring Mn_{12} units (>8.39 Å). The organic alkoxide and carboxylate bridging ligands oriented toward the center of the loop occupy the space of its central cavity and do not leave empty room for guest molecules; as a result, the lattice MeCN molecules are located above and below each loop.

Compound **1** joins the family of Mn_{12} wheels and is related to the subclass of complexes containing the general formula $[Mn_{12}(L)_8(RCO_2)_{14}]$, where L are N-substituted diethanolamine dianions.[28,30] As mentioned above, **1** consists of six Mn^{II} and six Mn^{III} ions, which is also the case in the latter Mn_{12} wheels; however, **1** is constructed by alternate Mn^{II}_2 and Mn^{III}_2 dimeric units instead of alternating Mn^{II} and Mn^{III} ions. Therefore, **1** is (a) only the second example of a 3d cluster bearing the mpt^{3-} ligand,[34] (b) the first example of a $Mn^{II}_6Mn^{III}_6$ wheel made of homovalent dimers, and (c) the first example of such a loop with the trigonal symmetry of a Reuleaux triangle, while the predecessor examples are all ellipsoids.

Magnetochemistry. Solid-state, variable-temperature magnetic susceptibility measurements were performed on a vacuum-dried microcrystalline sample of complex **1**·H_2O, which was suspended in eicosane to prevent torquing. The dc magnetic susceptibility (χ_M) data were collected in the 5.0−300 K range in a 0.1 T magnetic field and are plotted as $\chi_M T$ versus T in Figure 4. $\chi_M T$ gradually decreases during the whole

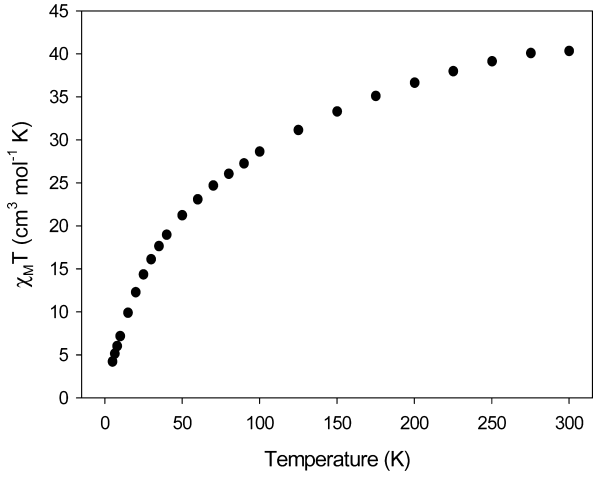

Figure 4. dc magnetic susceptibility of complex **1**, plotted as $\chi_M T$ versus T.

temperature range from 40.34 $cm^3\ mol^{-1}$ K at room temperature to 21.23 $cm^3\ mol^{-1}$ K at 50 K and then to 4.23 $cm^3\ mol^{-1}$ K at 5 K. The 300 K value is slightly lower than the spin-only (g = 2) value of 44.25 $cm^3\ mol^{-1}$ K for a complex consisting of six Mn^{II} and six Mn^{III} non-interacting ions, indicating the presence of dominant antiferromagnetic interactions within the molecule. This is also confirmed from the continuous decrease of the $\chi_M T$ value with decreasing temperature, which is heading for zero at the lowest temperatures, indicating that complex **1** possesses an S = 0 ground state. It is noted, however, that, for a singlet S = 0, the susceptibility is expected to approach zero at zero temperature, which may or may not be the case here. The reason for this caveat is 2-fold: (a) possible anisotropic effects could lead to a $\chi_M > 0$ behavior, as has been recently seen in the antiferromagnetic Fe_{18} wheel with a diamagnetic ground state;[47] (b) the presence of a highly dense manifold of excited states, only slightly above the ground state, and/or excited states that are more separated from the ground state but have S values greater than the ground state is present. The M_s levels of the latter drop in energy quite rapidly because of the applied magnetic field and approach (or even cross) those of the ground state.[15g] The case of low-lying excited states is also expected because of the high content of Mn^{II} ions in **1** (50% of the metal centers). Exchange interactions involving Mn^{II} ions are known to be very weak and almost always antiferromagnetic and usually lead to small energy separations even at the lowest temperatures, where the Boltzmann population of the excited states is normally expected to approach zero.[48] Given the size and complexity of the magnetic system, it was not possible to apply the Kambe method to determine the individual pairwise exchange interaction parameters between the Mn ions[49] or to easily use matrix diagonalization methods. The exchange parameters were therefore determined computationally using DFT methods (vide infra).

dx.doi.org/10.1021/ic401872c | *Inorg. Chem.* 2013, 52, 12070−12079

For an independent confirmation of the diamagnetic ground state, we carried out ac magnetic susceptibility studies on **1**·H_2O, which are a powerful complement to dc studies for determining the ground state of the system. As such, they preclude the various complications arising from the presence of a dc field.[50] Thus, the spin ground state $S = 0$ for complex **1** was further evidenced in ac magnetic susceptibility studies, performed between 1.8 and 15 K, using a 3.5 G ac field oscillating at frequencies in the 5−1500 Hz range. Figure 5 shows the in-phase component of the ac susceptibility for complex **1**, plotted as $\chi'_M T$ versus T, while the imaginary component of the susceptibility, as a χ''_M versus T plot, is available in the Supporting Information. The in-phase signal steadily decreases with decreasing temperature (the slope of the curve remains constant throughout the temperature range), indicating depopulation of one or more excited states as the temperature drops. Extrapolation of the in-phase plot to 0 K, where only the ground state is populated, gives a $\chi'_M T$ value of ~0.5 $cm^3\ mol^{-1}\ K$, instead of 0 $cm^3\ mol^{-1}\ K$, as would be expected for an $S = 0$ ground state. Thus, our initial prediction, from the dc data, of very low-lying excited states slightly above the singlet ground state for **1** is also confirmed by the ac magnetic susceptibility study. Finally, as expected, complex **1**·H_2O does not exhibit an out-of-phase ac signal down to 1.8 K (Figure S1, Supporting Information), and thus is not an SMM.

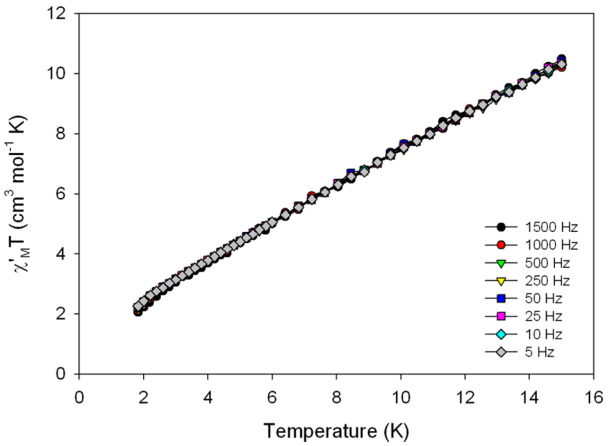

Figure 5. In-phase ac magnetic susceptibility of complex **1** as the $\chi'_M T$ versus T plot, with the 3.5G ac field oscillating at the indicated frequencies.

The physics of antiferromagnetic wheels is surprisingly rich because they were initially regarded as models of 1D antiferromagnetic chains; however, later theoretical and experimental work suggested that their physics cannot be accurately described as a classical antiferromagnetic Heisenberg ring,[20a] but the rotational or L- and E-band concept (quantum-mechanical effect) should be considered.[20b] Therefore, the availability of a new member of this small Mn_{12} single-stranded antiferromagnetic wheel family may shine light on complicated mesoscopic phenomena currently under investigation by the condensed-matter physics community.

Theoretical Studies. Compound **1** consists of dinuclear Mn^{II}_2 and Mn^{III}_2 units bridged by carboxylate and alkoxo ligands, which are known to often propagate antiferromagnetic interactions,[51] and thus the diamagnetic ground state was not a surprise. However, it was a matter of interest to determine the relative strength of the exchange parameters that lead to the $S = 0$ ground state. Unfortunately, compound **1** is not amenable to the Kambe method[49] because of its high nuclearity and the resulting number of inequivalent exchange parameters. Therefore, we obtained the J values from theoretical calculations using DFT methods.

Close inspection of the structure of **1** reveals the existence of four superexchange pathways, and thus four different exchange parameters J_i ($i = 1$−4) are required to model this spin system (Figure 6a): J_1 is the $Mn^{III}\cdots Mn^{III}$ interaction, i.e., the interaction of Mn2···Mn3 (and their symmetry-related partners) through two alkoxo bridges; J_2 is the $Mn^{II}\cdots Mn^{II}$ interaction, i.e., the interaction of Mn1 and its neighboring Mn4 (and their symmetry equivalent atoms) through two monatomic and one triatomic bridges from three different $CH_3CO_2^-$ ions; J_3 is the interaction of Mn1···Mn2 (and their

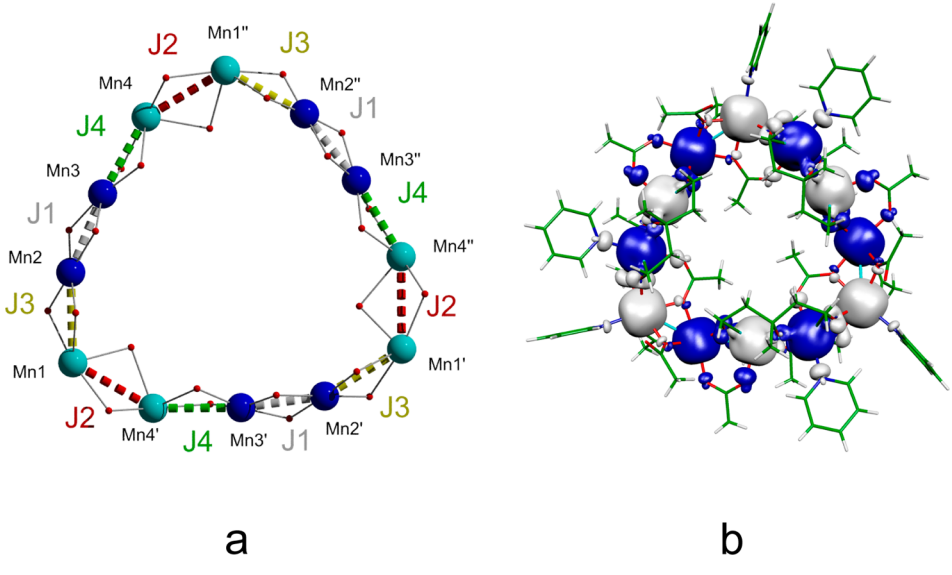

Figure 6. Representations of (a) the Mn/O core of complex **1** indicating the exchange parameters (J) employed in the theoretical calculations and (b) the spin-density map calculated at the B3LYP level for the singlet ground state of **1**. The isodensity surface presented corresponds to a value of 0.005 e $bohr^{-3}$. Blue and white regions indicate positive and negative spin populations, respectively.

dx.doi.org/10.1021/ic401872c | Inorg. Chem. 2013, 52, 12070−12079

symmetry equivalent atoms) through two alkoxo bridges and one μ_3 $CH_3CO_2^-$ ion; J_4 is associated with the interaction of Mn3···Mn4 (and their symmetry-related metal ions) through two alkoxo bridges and one μ carboxylate ion. Note that J_3 and J_4 both correspond to Mn^{II}···Mn^{III} interactions but with significant differences between the geometric characteristics of the Mn1···Mn2 and Mn3···Mn4 pairs that involve (i) different coordination numbers and geometries of the Mn^{III} ions (Mn2 ion is hexacoordinated, whereas Mn3 is pentacoordinated), (ii) different bridging modes adopted by the carboxylate ligands connecting the Mn^{III}–Mn^{II} ions (η^1:η^2:μ_3 vs η^1:η^1:μ coordination modes for the carboxylates connecting Mn1···Mn2 and Mn3···Mn4 ions, respectively), and (iii) different bond lengths. Concerning the last point, we note that the axial Mn^{III}–O_{ac} distance is ∼0.1 Å shorter in the case of the pentacoordinated Mn ion (2.114 vs 2.246 Å for Mn3 and Mn2 ions, respectively; see Table 4). The same trend is also observed for the Mn^{II}–O_{ac} distance (2.244 vs 2.167 for Mn1 and Mn4 ions, respectively; see Table 4).

Table 4. Structural Parameters in 1 Used in the DFT Study and the Calculated Exchange Coupling Parameters from Use of the B3LYP Hybrid Functional

	bridging ligands[a]	Mn···Mn (Å)	Mn–O (Å)[b]	Mn–O–Mn (deg)	J values
J_1	2 μ-OR	2.913	1.911, 1.913, 1.927, 1.937	98.7, 98.3	−34.3
J_2	2 μ-O_2CCH_3	3.274	2.131, 2.148, 2.244	98.7, 94.6	−4.5
	μ-O_2CCH_3		2.102, 2.167, 2.209		
J_3	2 μ-OR	3.084	2.165, 2.188, 2.244	99.6, 99.1	+1.2
	μ-O_2CCH_3		1.856, 1.865, 2.246		
J_4	2 μ-OR	3.069	2.181, 2.188, 2.167	98.7, 98.3	−4.3
	μ-O_2CCH_3		1.845, 1,867, 2.114		

[a]R = alkoxide of the mpt^{3-} backbone. [b]The underlined values correspond to structural parameters of the Mn^{II} cations.

The calculated J values using the B3LYP hybrid functional together with several structural parameters of **1** are presented in Table 4. Analysis of the results allows us to extract the following conclusions: (1) The J_1 exchange Mn^{III}···Mn^{III} interaction is antiferromagnetic and stronger than the J_2 Mn^{II}···Mn^{II} interaction, which is in excellent agreement with previously reported findings for Mn^{III}···Mn^{III} and Mn^{II}···Mn^{II} interactions.[52,53] (2) The J_3 exchange Mn^{II}···Mn^{III} interaction is the only one that is ferromagnetic, and its sign and value match perfectly with those calculated for a very similar pathway appearing in a member of the previously reported Mn_{12} family of wheels.[31a] (3) The J_4 exchange Mn^{II}···Mn^{III} interaction, although it corresponds to a pathway similar to that of J_3, is weakly antiferromagnetic. The existence of weak ferromagnetic (J_3) or antiferromagnetic (J_4) exchange interactions between Mn^{II} and Mn^{III} ions is consistent with the findings in several oligonuclear complexes containing $Mn^{II}Mn^{III}$ units, where the exchange interactions are either ferromagnetic or antiferromagnetic depending on the structural parameters and in all cases very weak.[54] The different signs of J_3 and J_4 are probably related to the appreciably shorter Mn^{III}–O_{ac} and Mn^{II}–O_{ac} bond lengths appearing in the superexchange pathway corresponding to antiferromagnetic coupling (J_4).[54]

The representation of the spin distribution corresponding to the most stable single-determinant wavefunction of **1** is plotted in Figure 6b. The opposite spin orientation in the Mn^{III}···Mn^{III} and Mn^{II}···Mn^{II} pairs is due to the antiferromagnetic intrapair couplings (J_1 and J_2), while the interpair interactions are either ferromagnetic (J_3) or antiferromagnetic (J_4). It is clearly impossible to fulfill all of the above-mentioned conditions at the same time; thus, one or more interactions are expected to be frustrated; the most stable S = 0 spin configuration corresponds to the case in which the weakest interaction (J_3) appears to be frustrated. The diagonalization of the matrix Hamiltonian is not possible because of large memory requirements. However, the relatively large stability of such a S = 0 singlet determinant is anticipated to give a singlet ground state for the complex. Spin distribution shows a predominance of spin delocalization of the Mn^{II} cations because they have unpaired electrons in all the d orbitals including those with antibonding character. Thus, the sign of the spin density in the neighboring ligand atoms is the same as that in the metal due to the metal–ligand orbital mixing of the antibonding orbitals. However, for the Mn^{III} centers in the xy plane, the spin polarization is the main mechanism of interaction; consequently, the sign of the neighboring atom density in the equatorial plane is opposite to that of the metal. Thus, theoretical studies suggest a diamagnetic spin ground state (S = 0) for **1**, supporting our conclusion from dc and ac magnetic susceptibility measurements.

■ CONCLUSIONS

The use of the anion mpt^{3-} in manganese carboxylate chemistry has provided access to the new $Mn^{II/III}_{12}$ single-stranded molecular wheel **1**·3CH_3CN comprising alternating Mn^{II}_2 and Mn^{III}_2 dimeric structural units. The arrangement of the Mn ions in **1** closely resembles a guitar plectrum or the Reuleaux triangle, the simplest Reuleaux polygon. In fact, the presence of homovalent dimers and the shape/symmetry of the Mn/O core are indeed the most significant structural differences between **1** and its predecessor Mn_{12} wheels; the latter are ellipsoid loops of alternating divalent and trivalent Mn ions.

dc and ac magnetic susceptibility measurements in **1** revealed dominant antiferromagnetic exchange interactions between the metal ions, resulting in a diamagnetic ground state, which was also confirmed by DFT calculations. From the DFT study, the J constants were determined, and all but one interactions were found to be antiferromagnetic; the exception was J for the interaction between the six-coordinate Mn^{III} ion and its neighboring Mn^{II}, which is weakly ferromagnetic.

Thus, **1** joins a small family of mixed-valent Mn wheels, which have previously induced a wave of scientific activity in the chemistry and condensed-matter physics communities; as such, the availability of a new mixed-valent Mn_{12} loop, with unprecedented structural characteristics and symmetry, is of particular significance. Furthermore, the fact that it possesses an S_T = 0 ground state makes it attractive for magnetochemists and physicists because antiferromagnetic wheels exhibiting a diamagnetic ground state, even though they are not SMMs, are still of interest because they can serve as effective models for monitoring Néel vector tunneling,and other relaxation mechanisms in antiferromagnetic systems.

Our continuing synthetic efforts toward the isolation of new clusters and/or metal−organic frameworks from the use of polyols has afforded a new Mn_{12} mixed-valent antiferromagnetic wheel, a new addition to a very small but quite interesting class of molecular systems. Our investigation of the H_3mpt ligand is ongoing, and the use of bulky carboxylates, different ligand combinations and the incorporation of other 3d and/or 4f metals are within the scope of the current project. Since the chemistry of polyols has been particularly rich, we have no reason to believe that this will not be the case for the H_3mpt ligand.

■ ASSOCIATED CONTENT

Supporting Information

Crystallographic data for complex **1** in CIF format and the out-of-phase susceptibility χ_M'' versus T plot (Figure S1). This material is available free of charge via the Internet at http://pubs.acs.org.

■ AUTHOR INFORMATION

Corresponding Author

*E-mail: atasio@ucy.ac.cy.

Present Address

[§]Department of Chemistry, Brock University, St. Catharines, L2S 3A1 Ontario, Canada.

Notes

The authors declare no competing financial interest.

■ ACKNOWLEDGMENTS

A.J.T., S.Z., and C.P. thank the Cyprus Research Promotion Foundation (Grants ΔΙΕΘΝΗΣ/ΣΤΟΧΟΣ/0308/14 and ΕΝΙΣΧ/0506/08). A.J.T. and C.P. are thankful for the European Union Seventh Framework Program (FP7/2007-2013) under Grants PCIG09-GA-2011-293814 and PIRSES-GA-2011-295190. E.C. and E.R. were supported by the Spanish Ministerio de Economía y Competitividad (Grant CTQ2011-23862-C02-01) and the regional Generalitat de Catalunya authority (Grant 2009SGR-1459). C.L. acknowledges the University of North Florida for the summer faculty development grant and the Chemistry Department at the University of Cyprus for providing him the visiting professorship appointment. G.C. acknowledges the National Science Foundation (Grant DMR-1213030). The authors thankfully acknowledge the computer resources, technical expertise, and assistance provided by the Barcelona Supercomputer Center.

■ REFERENCES

(1) Gatteschi, D.; Sessoli, R.; Villain, J. *Molecular Nanomagnets*; Oxford University Press: Oxford, U.K., 2007.

(2) (a) Lippard, S. J.; Berg, J. M. *Principles of Bioinorganic Chemistry*; University Science Books: Mill Valley, CA, 1994. (b) Ochiai, E.-I. *Bioinorganic Chemistry: A Survey*, 1st ed.; Elsevier Science Publishing Co.: San Diego, CA, 2008.

(3) (a) Ohki, Y.; Tatsumi, K. *Z. Anorg. Allg. Chem.* **2013**, *639*, 1340. (b) Malinak, S. M.; Coucouvanis, D. *Prog. Inorg. Chem.* **2001**, *49*, 599. (c) Holm, R. H.; Armstrong, W. H.; Christou, G.; Mascharak, P. K.; Mizobe, Y.; Palermo, R. E.; Yamamura, T. In *Biomimetic Chemistry*; Yoshida, Z. I., Ise, N., Eds.; Elsevier: New York, 1983.

(4) (a) Gorun, S. M.; Lippard, S. J. *Nature* **1986**, *319*, 666. (b) Muller, A.; Rehder, D. In *Coordination Chemistry in Protein Cages: Principles, Design, and Applications*, 1st ed.; Ueno, T., Watanabe, Y., Eds.; John Wiley & Sons: New York, 2013.

(5) (a) Sauer, K.; Yano, J.; Yachandra, V. K. *Coord. Chem. Rev.* **2008**, *252*, 318 and references cited therein. (b) Mukherjee, S.; Stull, J. A.; Yano, J.; Stamatatos, T. C.; Pringouri, K.; Stich, T. A.; Abboud, K. A.; Britt, R. D.; Yachandra, V. K.; Christou, G. *Proc. Natl. Acad. Sci. U.S.A.* **2012**, *109*, 2257. (c) Koumousi, E. S.; Mukherjee, S.; Beavers, C. M.; Teat, S. J.; Christou, G.; Stamatatos, T. C. *Chem. Commun.* **2011**, *47*, 11128. (d) Kanady, J. S.; Tsui, E. Y.; Day, M. W.; Agapie, T. *Science* **2011**, *333*, 733.

(6) (a) Bagai, R.; Christou, G. *Chem. Soc. Rev.* **2009**, *38* (4), 1011 and references cited therein.. (b) Christou, G.; Gatteschi, D.; Hendrickson, D. N.; Sessoli, R. *MRS Bull.* **2000**, *25*, 66. (c) Aromi, G.; Brechin, E. K. *Struct. Bonding (Berlin)* **2006**, *122*, 1 and references cited therein.

(7) Bogani, L.; Wernsdorfer, W. *Nat. Mater.* **2008**, *7*, 179.

(8) (a) Hill, S.; Edwards, R. S.; Aliaga-Alcalde, N.; Christou, G. *Science* **2003**, *302*, 1015−1018. (b) Tiron, R.; Wernsdorfer, W.; Foguet-Albiol, D.; Aliaga-Alcalde, N.; Christou, G. *Phys. Rev. Lett.* **2003**, *91*, 227203(1−4).

(9) (a) Kovalev, A.; Hayden, L.; Bauer, G.; Tscherkovniak, Y. *Phys. Rev. Lett.* **2011**, *106*, 147203. (b) Garanin, D. A.; Chudnovsky, E. *Phys. Rev. X* **2011**, *1*, 011005. (c) Ganzhorn, M.; Klyatskaya, S.; Ruben, M.; Wernsdorfer, W. *Nat. Nanotechnol.* **2013**, *8*, 166.

(10) (a) Wernsdorfer, W.; Bhaduri, S.; Boskovic, C.; Christou, G.; Hendrickson, D. N. *Phys. Rev. B* **2002**, *65*, 180403. (b) Wernsdorfer, W.; Chakov, N. E.; Christou, G. *Phys. Rev. Lett.* **2005**, *95*, 037203.

(11) (a) Gatteschi, G.; Sessoli, R. *Angew. Chem., Int. Ed.* **2003**, *42*, 268. (b) del Barco, E.; Kent, A. D.; Hill, S.; North, J. M.; Dalal, N. S.; Rumberger, E. M.; Hendrickson, D. N.; Chakov, N. E.; Christou, G. *J. Low Temp. Phys.* **2005**, *140*, 119. (c) Stamp, P. C. E. *Nature* **1996**, *383*, 125.

(12) (a) Wernsdorfer, W.; Sessoli, R. *Science* **1999**, *284*, 133. (b) Wernsdorfer, W.; Soler, M.; Christou, G.; Hendrickson, D. N. *J. Appl. Phys.* **2002**, *91*, 7164.

(13) (a) Macia, F.; Hernandez, J. M.; Tejada, J.; Datta, S.; Hill, S.; Lampropoulos, C.; Christou, G. *Phys. Rev. B* **2009**, *79*, 092403. (b) Adams, S. T.; da Silva Neto, E. H.; Datta, S.; Ware, J. F.; Lampropoulos, C.; Christou, G.; Myaesoedov, Y.; Zeldov, E.; Friedman, J. R. *Phys. Rev. Lett.* **2013**, *110*, 087205.

(14) (a) Tasiopoulos, A. J.; Vinslava, A.; Wernsdorfer, W.; Abboud, K. A.; Christou, G. *Angew. Chem., Int. Ed.* **2004**, *43*, 2117. (b) Manoli, M.; Inglis, R.; Manos, M. J.; Nastopoulos, V.; Wernsdorfer, W.; Brechin, E. K.; Tasiopoulos, A. J. *Angew. Chem., Int. Ed.* **2011**, *50*, 4441. (c) Manoli, M.; Prescimone, A.; Mishra, A.; Parsons, S.; Christou, G.; Brechin, E. K. *Dalton Trans.* **2007**, 532. (d) Scott, R. T. W.; Milios, C. J.; Vinslava, A.; Lifford, D.; Parsons, S.; Wernsdorfer, W.; Christou, G.; Brechin, E. K. *Dalton Trans.* **2006**, 3161. (e) Moushi, E. E.; Lampropoulos, C.; Wernsdorfer, W.; Nastopoulos, V.; Christou, G.; Tasiopoulos, A. J. *J. Am. Chem. Soc.* **2010**, *132*, 16146. (f) Moushi, E. E.; Lampropoulos, C.; Wernsdorfer, W.; Nastopoulos, V.; Christou, G.; Tasiopoulos, A. J. *Inorg. Chem.* **2007**, *46*, 3795. (g) Charalambous, M.; Moushi, E. E.; Papatriantafyllopoulou, C.; Wernsdorfer, W.; Nastopoulos, V.; Christou, G.; Tasiopoulos, A. J. *Chem. Commun.* **2012**, *48*, 5410. (h) Manoli, M.; Prescimone, A.; Bagai, R.; Mishra, A.; Murugesu, M.; Parsons, S.; Wernsdorfer, W.; Christou, G.; Brechin, E. K. *Inorg. Chem.* **2007**, *46*, 6968. (i) Nguen, T. N.; Wernsdorfer, W.; Abboud, K. A.; Christou, G. *J. Am. Chem. Soc.* **2011**, *133*, 20688. (j) Foguet-Albiol, D.; Abboud, K. A.; Christou, G. *Chem. Commun.* **2005**, 4282.

(15) (a) Murugesu, M.; Wernsdorfer, W.; Abboud, K. A.; Christou, G. *Angew. Chem., Int. Ed.* **2005**, *44*, 892. (b) Liu, W.; Lee, K.; Park, M.; John, R. P.; Moon, D.; Zou, Y.; Liu, X.; Ri, H.-C.; Kim, G. H.; Lah, M. S. *Inorg. Chem.* **2008**, *47*, 8807. (c) Ramsey, C. M.; Heroux, K. J.; O'Brien, J. R.; DiPasquale, A. G.; Rheingold, A. L.; del Barco, E.; Hendrickson, D. N. *Inorg. Chem.* **2008**, *47*, 6245. (d) Crewdson, P.; Gambarotta, S.; Yap, G. P. A.; Thompson, L. K. *Inorg. Chem.* **2003**, *42*, 8579. (e) Timco, G. A.; Faust, T. B.; Tuna, F.; Winpenny, R. E. P. *Chem. Soc. Rev.* **2011**, *40*, 3067 and references cited therein. (f) Engelhardt, L. P.; Muryn, C. A.; Pritchard, R. G.; Timco, G. A.; Tuna, F.; Winpenny, R. E. P. *Angew. Chem., Int. Ed.* **2008**, *47*, 924. (g) Lampropoulos, C.; Stamatatos, T. C.; Abboud, K. A.; Christou, G. *Polyhedron* **2009**, *28*, 1958. (h) Stamatatos, T. C.; Vlahopoulou, G.;

Raptopoulou, C. P.; Psycharis, V.; Esquer, A.; Christou, G.; Perlepes, S. P. *Eur. J. Inorg. Chem.* **2012**, 3121. (i) Timco, G. A.; McInnes, E. J. L.; Winpenny, R. E. P. *Chem. Soc. Rev.* **2013**, *42*, 1796 and references cited therein.

(16) Cornia, A.; Jansen, A. G. M.; Affronte, M. *Phys. Rev. B* **1999**, *60*, 12177.

(17) (a) Chiolero, A.; Loss, D. *Phys. Rev. Lett.* **1998**, *80*, 169. (b) Meier, F.; Loss, D. *Phys. Rev. B* **2001**, *64*, 224411. (c) Meier, F.; Loss, D. *Phys. Rev. Lett.* **2001**, *86*, 5373. (d) Waldmann, O.; Stamatatos, T. C.; Christou, G.; Gudel, H. U.; Sheikin, I.; Mutka, H. *Phys. Rev. Lett.* **2009**, *102*, 157202.

(18) Meier, F.; Loss, D. *Phys. B* **2003**, *329*, 1140.

(19) Kahn, O. *Molecular Magnetism*; VCH Publishers: New York, 1993.

(20) (a) Furrer, A.; Waldmann, O. *Rev. Mod. Phys.* **2013**, *85*, 367 and references cited therein. (b) Waldmann, O. *Coord. Chem. Rev.* **2005**, *249*, 2550 and references cited therein..

(21) Cador, O.; Gatteschi, D.; Sessoli, R.; Barra, A.-L.; Timco, G. A.; Winpenny, R. E. P. *J. Magn. Magn. Mater.* **2005**, *290*, 55.

(22) (a) Dechambenoit, P.; Long, J. R. *Chem. Soc. Rev.* **2011**, *40*, 3249 and references cited therein. (b) Saalfrank, R. W.; Maid, H.; Scheurer, A. *Angew. Chem., Int. Ed.* **2008**, *47*, 8794 and references cited therein.

(23) (a) Kumagai, H.; Kitagawa, S. *Chem. Lett.* **1996**, 471. (b) Chen, Y.; Liu, Q.; Deng, Y.; Zhu, H.; Chen, C.; Fan, H.; Liao, D.; Gao, E. *Inorg. Chem.* **2001**, *40*, 3723.

(24) Affronte, M.; Carretta, S.; Timco, G. A.; Winpenny, R. E. P. *Chem. Commun.* **2007**, 1789 and references cited therein.

(25) Liu, W.; Lee, K.; Park, M.; Hohn, R. P.; Moon, D.; Zou, Y.; Liu, X.; Ri, H.-C.; Kim, G. H.; Lah, M. S. *Inorg. Chem.* **2008**, *47*, 8807 and references cited therein.

(26) (a) Taft, K. L.; Delfs, C. D.; Papaefthymiou, G. C.; Foner, S.; Gatteschi, D.; Lippard, S. J. *J. Am. Chem. Soc.* **1994**, *116*, 823. (b) Benelli, C.; Parsons, S.; Solan, G. A.; Winpenny, R. E. P. *Angew. Chem., Int. Ed.* **1996**, *35*, 1825. (c) McInnes, E. J. L.; Anson, C.; Powell, A. K.; Thomson, A. J.; Poussereau, S.; Sessoli, R. *Chem. Commun.* **2001**, 89. (d) Cañada-Vilalta, C.; Pink, M.; Christou, G. *Chem. Commun.* **2003**, 1240. (e) Frey, M.; Harris, S. G.; Holmes, J. M.; Nation, D. A.; Parsons, S.; Tasker, P. A.; Teat, S. J.; Winpenny, R. E. P. *Angew. Chem., Int. Ed.* **1998**, *37*, 3246. (f) Waldmann, O.; Schülein, J.; Koch, R.; Müller, P.; Bernt, I.; Saalfrank, R. W.; Andres, H. P.; Guldel, H. U.; Allenspach, P. *Inorg. Chem.* **1999**, *38*, 5879. (g) Saalfrank, R. W.; Bernt, I.; Chowdhry, M. M.; Hampel, F.; Vaughan, G. B. N. *Chem.—Eur. J.* **2001**, *7*, 2765. (h) Jones, L. F.; Batsanov, A.; Brechin, E. K.; Collison, D.; Helliwell, M.; Mallah, T.; McInnes, E. J. L.; Piligkos, S. *Angew. Chem., Int. Ed.* **2002**, *41*, 4318. (i) Abu-Nawwas, A.-A. H.; Cano, J.; Christian, P.; Mallah, T.; Rajaraman, G.; Teat, S. J.; Winpenny, R. E. P.; Yukawa, Y. *Chem. Commun.* **2004**, 314. (j) Lin, S.; Liu, S.-X.; Chen, Z.; Lin, B.-Z.; Gao, S. *Inorg. Chem.* **2004**, *43*, 2222. (k) Stamatatos, T. C.; Christou, A. G.; Mukherjee, S.; Poole, K. M.; Lampropoulos, C.; Abboud, K. A.; O'Brien, T. A.; Christou, G. *Inorg. Chem.* **2008**, *47*, 9021. (l) Stamatatos, T. C.; Christou, A. G.; Jones, C. M.; O'Callaghan, B.; Abboud, K. A.; O'Brien, T. A.; Christou, G. *J. Am. Chem. Soc.* **2007**, *129*, 9840.

(27) (a) Stamatatos, T. C.; Mukherjee, S.; Abboud, K. A.; Christou, G. *Chem. Commun.* **2009**, 62. (b) King, P.; Stamatatos, T. C.; Abboud, K. A.; Christou, G. *Angew. Chem., Int. Ed.* **2006**, *45*, 7379. (c) Papaefstathiou, G. S.; Manessi, A.; Raptopoulou, C. P.; Terzis, A.; Zafiropoulos, T. F. *Inorg. Chem.* **2006**, *45*, 8823.

(28) Foguet-Albiol, D.; O'Brien, T. A.; Wernsdorfer, W.; Moulton, B.; Zaworotko, M. J.; Abboud, K. A.; Christou, G. *Angew. Chem., Int. Ed.* **2005**, *44*, 897.

(29) (a) Stamatatos, T. C.; Abboud, K. A.; Wernsdorfer, W.; Christou, G. *Angew. Chem., Int. Ed.* **2008**, *47*, 6694. (b) Manoli, M.; Prescimone, A.; Bagai, R.; Mishra, A.; Murugesu, M.; Parsons, S.; Wernsdorfer, W.; Christou, G.; Brechin, E. K. *Inorg. Chem.* **2007**, *46*, 6968. (c) Shah, S. J.; Ramsey, C. M.; Heroux, K. J.; O'Brien, J. R.; DiPasquale, A. G.; Rheingold, A. L.; del Barco, E.; Hendrickson, D. N. *Inorg. Chem.* **2008**, *47*, 6245.

(30) (a) Rumberger, A. M.; Zakharov, L. N.; Rheingold, A. L.; Hendrickson, D. N. *Inorg. Chem.* **2004**, *43*, 6531. (b) Rumberger, A. M.; Shah, S. J.; Beedle, C. C.; Zakharov, L. N.; Rheingold, A. L.; Hendrickson, D. N. *Inorg. Chem.* **2005**, *44*, 2742. (c) Shah, S. J.; Ramsey, C. M.; Heroux, K. J.; DiPasquale, A. G.; Dalal, N. S.; Rheingold, A. L.; del Barco, E.; Hendrickson, D. N. *Inorg. Chem.* **2008**, *47*, 9569.

(31) (a) Cano, J.; Costa, R.; Alvarez, S.; Ruiz, E. *J. Chem. Theory Comput.* **2007**, *3*, 782. (b) Gangopadhyay, S.; Masunov, A. E.; Poalelungi, E.; Leuenberger, M. N. *J. Chem. Phys.* **2010**, *132*, 244104.

(32) Ramsey, C. M.; del Barco, E.; Hill, S.; Shah, S. J.; Beedle, C. C.; Hendrickson, D. N. *Nat. Phys.* **2008**, *4*, 277.

(33) Wernsdorfer, W.; Stamatatos, T. C.; Christou, G. *Phys. Rev. Lett.* **2008**, *101*, 237204.

(34) (a) Nayak, S.; Evangelisti, M.; Powell, A. K.; Reedijk, J. *Chem.—Eur. J.* **2010**, *16*, 12865. (b) Stuiber, S.; Wu, G.; Nehkorn, J.; Dreiser, J.; Lan, Y.; Novitchi, G.; Anson, C. E.; Unruh, T.; Powell, A. K.; Waldmann, O. *Chem.—Eur. J.* **2011**, *17*, 9094.

(35) *CrysAlis CCD and CrysAlis RED*, version 1.171.32.15; Oxford Diffraction Ltd.: Abingdon, Oxford, England, 2008.

(36) (a) *SIR92*: Altomare, A.; Cascarano, G.; Giaconazzo, C.; Guagliardi, A.; Burla, M. C.; Polidori, G.; Camalli, M. *J. Appl. Crystallogr.* **1994**, *27*, 435. (b) Sheldrick, G. M. *SHELXL97*; University of Göttingen: Göttingen, Germany, 1997. (c) Farrugia, L. J. *J. Appl. Crystallogr.* **1999**, *32*, 837.

(37) (a) Brandenburg, K. *DIAMOND*, version 3.1d; Crystal Impact GbR: Bonn, Germany, 2006. (b) Macrae, C. F.; Edgington, P. R.; McCabe, P.; Pidcock, E.; Shields, G. P.; Taylor, R.; Towler, M.; Van de Streek, J. *J. Appl. Crystallogr.* **2006**, *39*, 453.

(38) Ruiz, E.; Rodriguez-Fortea, A.; Cano, J.; Alvarez, S.; Alemany, P. *J. Comput. Chem.* **2003**, *24*, 982.

(39) (a) Ruiz, E.; Rodriguez-Fortea, A.; Tercero, J.; Cauchy, T. J. *Chem. Phys.* **2005**, *123*, 074102. (b) Ruiz, E. *Struct. Bonding (Berlin)* **2004**, *113*, 71.

(40) Becke, A. D. *J. Chem. Phys.* **1993**, *98*, 5648.

(41) Valiev, M.; Bylaska, E. J.; Govind, N.; Kowalski, K.; Straatsma, T. P.; van Dam, H. J. J.; Wang, D.; Nieplocha, J.; Apra, E.; Windus, T. L.; de Jong, W. A. *Comput. Phys. Commun.* **2010**, *181*, 1477.

(42) *Jaguar7.5*; Schrödinger, Inc.: New York, 2009.

(43) Schaefer, A.; Huber, C.; Ahlrichs, R. J. *Chem. Phys.* **1994**, *100*, 5829.

(44) (a) Moushi, E. E.; Stamatatos, T. C.; Wernsdorfer, W.; Nastopoulos, V.; Christou, G.; Tasiopoulos, A. J. *Inorg. Chem.* **2009**, *48*, 5049. (b) Moushi, E. E.; Stamatatos, T. C.; Wernsdorfer, W.; Nastopoulos, V.; Christou, G.; Tasiopoulos, A. J. *Angew. Chem., Int. Ed.* **2006**, *45*, 7722. (c) Tasiopoulos, A. J.; Perlepes, S. P. *Dalton Trans.* **2008**, 5537.

(45) (a) Griffiths, D.; Culpin, D. *Mathl. Gaz.* **1975**, *59*, 165. (b) Ball, D. G. *Mathl. Gaz.* **1973**, *57*, 298.

(46) (a) Brown, I. D.; Altermatt, D. *Acta Crystallogr.* **1985**, *B41*, 244. (b) Liu, W.; Thorp, H. H. *Inorg. Chem.* **1993**, *32*, 4102.

(47) Ummethum, J.; Nehrkorn, J.; Mukherjee, S.; Ivanov, N. B.; Stuiber, S.; Strässle, Th.; Tregenna-Pigott, P. L. W.; Mutka, H.; Christou, G.; Waldmann, O.; Schnack, J. *Phys. Rev. B* **2012**, *86*, 104403.

(48) (a) Lampropoulos, C.; Murugesu, M.; Abboud, K. A.; Christou, G. *Polyhedron* **2007**, *26*, 2129. (b) Lampropoulos, C.; Koo, C.; Hill, S. O.; Abboud, K. A.; Christou, G. *Inorg. Chem.* **2008**, *47*, 11180.

(49) Kambe, K. *J. Phys. Soc. Jpn.* **1950**, *5*, 48.

(50) (a) Lampropoulos, C.; Stamatatos, T. C.; Manos, M. J.; Tasiopoulos, A. J.; Abboud, K. A.; Christou, G. *Eur. J. Inorg. Chem.* **2010**, 2244. (b) Milios, C. J.; Raptopoulou, C. P.; Terzis, A.; Lloret, F.; Vicente, R.; Perlepes, S. P.; Escuer, A. *Angew. Chem., Int. Ed.* **2004**, *43*, 210. (c) Milios, C. J.; Vinslava, A.; Whittaker, A.; Parsons, S.; Wernsdorfer, W.; Perlepes, S. P.; Christou, G.; Brechin, E. K. *Inorg. Chem.* **2006**, *45*, 5272.

(51) Stamatatos, T. C.; Christou, G. *Philos. Trans. R. Soc.* **2008**, *366*, 113 and references cited therein.

(52) Cremades, E.; Cauchy, T.; Cano, J.; Ruiz, E. *Dalton Trans.* **2009**, 5873.
(53) (a) Berg, N.; Rajeshkumar, T.; Taylor, S. M.; Brechin, E. K.; Rajaraman, G.; Jones, L. F. *Chem.—Eur. J.* **2012**, *18*, 5906. (b) Paine, T. K.; Weyhermüller, T.; Bothe, E.; Wieghardt, K.; Chaudhuri, P. *Dalton Trans.* **2003**, 3136.
(54) Manda, D.; Chatterjee, P. B.; Bhattacharya, S.; Choi, K. Y.; Clérac, R.; Chaudhury, M. *Inorg. Chem.* **2009**, *48*, 1826.